ASSESSMENT ON FATIGUE BEHAVIOUR OF AL7475 T7351 SUBJECTED TO NATURAL CORROSION, ACCELERATED CORROSION AND ARTIFICIAL DAMAGES

Daniele Mezzanzanica[1(*)], Giuseppe Ratti[1], Andrea Baldi[1], Ugo Mariani[1]
Marco Giglio[2], Andrea Manes[2], Marco Ormellese[3], Andrea Brenna[3]

[1]Leonardo Helicopter Division (LHD), via Giovanni Agusta 520, Cascina Costa (VA), Italy
[(*)]daniele.mezzanzanica@leonardo.com
[2]Politecnico di Milano, Dipartimento di Meccanica, via La Masa 1, Milano 20155, Italy
[3]Politecnico di Milano, Dipartimento di Chimica, Materiali e Ingegneria Chimica "G. Natta", via L. Mancinelli 7, Milano 20131, Italy

Abstract: Helicopter components can be subjected to possible in-service corrosion due to environmental operating conditions, controlled thought the adoption of protective coatings and dedicated inspection plans. Into the mainstream of Leonardo Helicopters plan, for European Plan for Aviation Safety 2020-2024 on 'ageing of the fleet', this research activity is focused on experimental activities devoted to evaluate the fatigue material behaviour in presence of several kind of corrosion pits, either from accelerated and natural corrosion, with the final objective to identify a correlation with artificial defects made by Electrical Discharge Machining (EDM), when subjected to fatigue loads. More specifically, in the context of damage tolerance assessment, the analysis focuses on the evaluation of threshold to propagation of small cracks emanating from either corrosion pits or EDM notch; the crack growth threshold and the fatigue endurance limit are combined through the Kitagawa-Takahashi diagram, defining the area of non-propagating cracks. Kitagawa-Takahashi is usually based on the crack length; the fatigue strength of metallic materials in the presence of small defects are well predicted applying the √area parameter model proposed by Murakami and Endo. Experimental activities have been performed on Aluminium Alloy 7475 T7351 in alternate bending, in presence of a defect with √area = 0.445 mm, equivalent to a semi-circular flaw of 0.35 mm radius. Evaluated defects are EDM notch, accelerated corrosion pits from galvanostatic and salt spray techniques, natural corrosion from exposition in urban and in marine environments. An ad-hoc galvanostatic procedure has been developed to promote a localized corrosive electrochemical attack. EDM notch, well-known for shape, size and technological process, are considered as a base case study and accelerated corrosion pits were generated to obtain the same value of √area.
The results of the activity show a strong correlation among the threshold to propagation from accelerated corrosion, natural corrosion and the artificial flaws obtained by EDM technique confirming the applicability of Kitagawa diagrams derived from EDM notches to describe the damage tolerance behaviour in presence of corrosion pits with equivalent size.

Keywords: Fatigue, Corrosion, EDM, Damage Tolerance, Al7475

INTRODUCTION

Corrosion is one of the most important threats which needs to be considered as source of accidental damage for the fatigue tolerance evaluation of susceptible metallic parts. Corrosion adversely impacts the structural integrity of aircraft, reducing the fatigue strength up to a level which may result catastrophic if not mitigated through a combined plan involving the evaluation of its effect on the fatigue strength correlated to a suitable inspection program. This research activity aims to correlate the fatigue material behaviour in presence of a corrosion pit, either from natural and accelerated corrosion, with results from artificial defects made by Electrical Discharge Machining (EDM), when subjected to fatigue loads. Corrosion pits act as a pre-existing flaws in the material, for the nucleation of fatigue cracks. While corrosion fatigue describes the material cracking under a combination of electrochemical and mechanical activity acting simultaneously, the present study is focused on cases where the two driving forces act separately, therefore cyclic loading is applied to a corrosion defect in inert environment. Stable pit growth is usually considered a time-dependent phenomenon and mainly controlled by electrochemical activity. Compared to pitting, cracking is predominantly a mechanical, fatigue cycle-dependent regime, although in the early stages of crack growth local crack tip chemistry is also a key condition to the development and propagation of small fatigue cracks [1]. The present activity evaluates the effect of corrosion pits on the fatigue strength, tested in inert environment.
In particular, the activity is focused on evaluating the conditions of threshold to propagation of small cracks emanating from either corrosion pits or EDM flaw. In this field, the Kitagawa-Takahashi diagram [2] is used. The Kitagawa-Takahashi combines the fatigue crack growth threshold and the fatigue endurance limit into a single plot, defining the area of non-propagating cracks; for cracks of given length and stress range it allows to predict the allowable stress range for infinite life [3]. Kitagawa- Takahashi is usually based on the crack length; it has been demonstrated that the fatigue strength of metallic materials in the presence of small defects is well predicted applying the √area parameter model proposed by Murakami and Endo [4].
Artificial defects generated on laboratory specimens to simulate the presence of a corrosion pit and to study the fatigue life was the approach used also by Smith et al. [5], which conducted uniaxial fatigue tests to compare the fatigue life of laboratory produced corrosion pits, similar to those observed in the shuttle main landing gear wheel bolt-hole, and an EDM flaw. Schonbauer et al. [6], [7] evaluated that corrosion pits can be treated as effective cracks by using the √area parameter model.
Comparison among the effect of accelerated and natural corrosion on fatigue life is not yet well investigated in the literature. Li et al. [8] assessed the effect of corrosion on the fatigue life of steel bars. Amount of corrosion is characterized as mass loss, while fatigue tests were performed in an inert environment.

Kitagawa-Takahashi Diagram

The fatigue limit of metallic materials used in aeronautical industry with micro-cracks or defects assumes a different meaning to that used in traditional safe-life concepts, and it can be considered to be the threshold stress for non-propagation of cracks emanating from original defects, being the nucleation phase not present alone but joined to the propagation phase. Using LEFM concepts, the general law which defines the fatigue limit of a cracked material is defined in Eqn. 1.

$$\Delta\sigma_{th} = \frac{\Delta \boldsymbol{K_{th}}}{\boldsymbol{Y} \cdot \sqrt{\boldsymbol{\pi a}}} \tag{1}$$

where ΔK_{th} is the threshold of the intensity factor for crack propagation, a is the crack length, and Y a geometry factor. Considering ΔK_{th} as a material property, Eqn. 1 is represented by a horizontal straight line on a log-log plot (Figure 1); tests carried out on materials with different initial crack sizes showed that this line is valid beyond a certain crack length whose value depends on the material, while for shorter cracks $\Delta\sigma_{th}$ is over-predicted. From Eqn. 1, this means that the value of ΔK_{th} reduces with reducing crack size and for short cracks, becoming also a function of the micro structure of the material, as shown in Figure 1, from ref. [9].

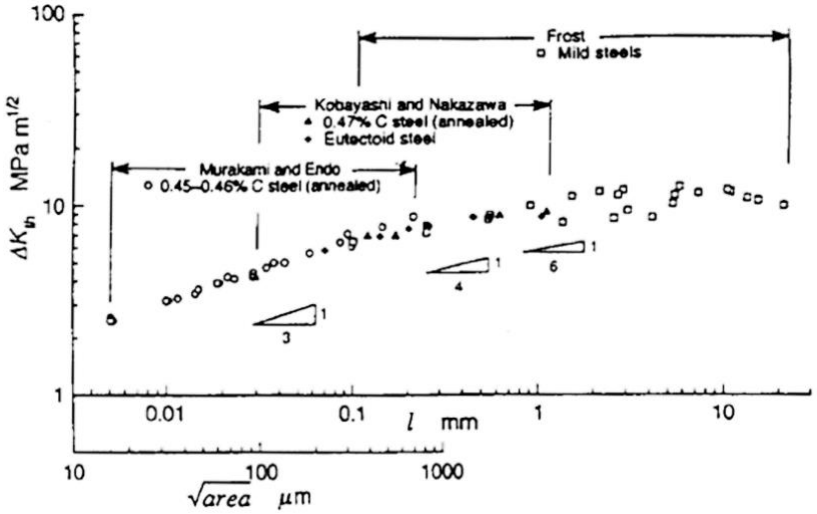

Figure 1: Dependence of ΔK_{th} on Crack or Defect Size [9]

Figure 2 shows the crack size effect on $\Delta\sigma_{th}$; the horizontal straight line is the fatigue limit of pristine specimens $\Delta\sigma_e$, the slant straight line is the $\Delta\sigma_{th}$ for $\Delta K_{th,\,lc}$ constant (Eqn. 1) These two lines represent an ideal behaviour and are called Smith's model [10], and they intersect at a crack size $a_{0,H}$ which is called the El-Haddad Parameter, expressed by Eqn. 2:

$$a_{0,H} = \frac{1}{\pi}\left(\frac{\Delta \boldsymbol{K_{th,lc}}}{\boldsymbol{Y}\cdot\Delta\boldsymbol{\sigma_e}}\right)^{\mathbf{2}} \tag{2}$$

where, for a given material, $\Delta K_{th,lc}$ denotes the fatigue threshold stress intensity factor range for long cracks, $\Delta\sigma_e$ the fatigue limit range of smooth specimens, and Y is the geometry factor of the crack [3]. Using the fictitious intrinsic crack length $a_{0,H}$ introduced by El Haddad [11], a smooth transition from the threshold of long cracks to the endurance limit is given defining the area of non-propagating cracks [3].
The smooth curve, known as the Kitagawa – Takahashi diagram, Kitagawa plot or Tanaka's model, is the upper limit of micro-crack growth varying the applied stress.

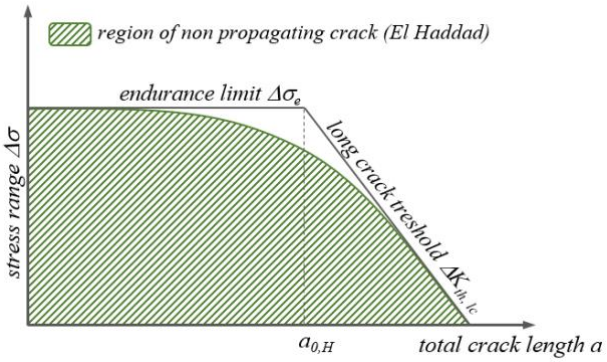

Figure 2: Kitagawa–Takahashi Diagram

The model which describes this plot is called El-Haddad's model and is expressed by Eqn. 3 [10]:

$$\Delta\sigma_{th} = \frac{\Delta \boldsymbol{K_{th}}}{\boldsymbol{Y}\cdot\sqrt{\boldsymbol{\pi}(\boldsymbol{a}+\boldsymbol{a_0})}} \tag{3}$$

The amplitude σ_w, in the presence of a small crack or defect can be derived by substituting the stress intensity factor range by its threshold, obtaining Eqn. 4:

$$\sigma_w = \sigma_e \sqrt{\frac{\boldsymbol{a_0}}{\boldsymbol{a + a_0}}} \qquad (4)$$

The √area parameter model proposed by Murakami and Endo

The defect tolerant fatigue design is usually based on the assumption that defects can be treated as effective cracks, consequently, the fatigue limit is correlated with the threshold for crack propagation. Eqn. 4 works properly for two-dimensional defects; it has been demonstrated that the fatigue strength of metallic materials in the presence of small defects can be well predicted applying the √area parameter model proposed by Murakami and Endo [4], defined as the square root of the area obtained by projecting a defect or a crack onto the plane perpendicular to the maximum tensile stress, as shown into Figure 3.

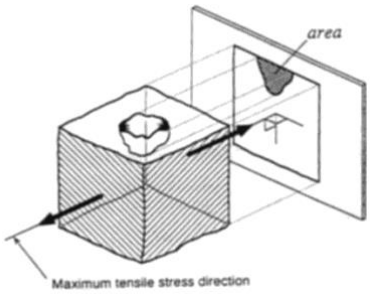

Figure 3:Definition of √area Parameter

Murakami made some considerations in the calculation of the effective value of √area of the defect [10]; for irregularly shaped cracks, an effective √area is estimated by considering a smooth contour which envelopes the original irregular shape.

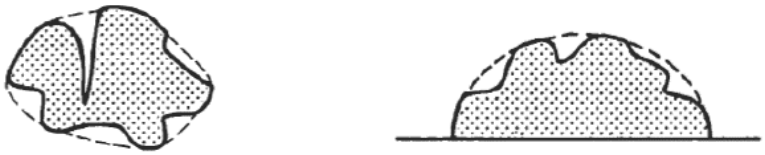

Figure 4: Irregularly Shaped Cracks

For very slender cracks, as shown in Figure 2-3, the effective √area is evaluated by truncating the slender shape to a limiting length, since the stress intensity factor tends to a constant value as the crack length increases, even though the √area increases without limit. The boundary limits used to estimate effective √area for the very shallow cracks (length/depth ≥10) and the very deep crack (depth/length ≥ 2.5) are detailed in Figure 5.

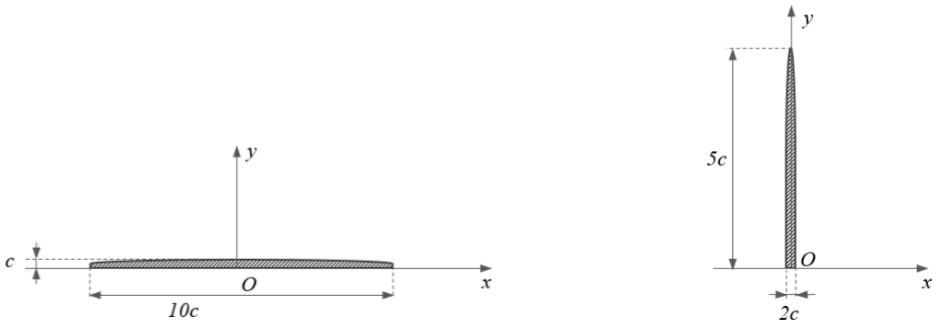

a) Very Shallow Surface Flaw Boundary Limit *b) Very Deep Surface Flaw Boundary Limit*

Figure 5: Very Deep and Shallow Flaws Boundary Limits

In the literature several works exploits the √area parameter model [12] [13] [6] [14]. Schonbauer et al. [12] performed fatigue tests up to the Very High Cycle Fatigue regime with specimens containing different kind of defects on precipitation-hardened chromium-nickel-copper stainless steel 17-4PH. The results were compared with data obtained from tests on smooth specimens in which failures mostly originated at non-metallic inclusions. It was found that the fatigue limit in the presence of small intrinsic or artificial defects can be predicted using the √area parameter model, which comprises the size dependency of the threshold stress intensity factor range. For larger defects with a sharp notch root radius, the fatigue limit can be estimated using the constant value for the threshold stress intensity factor range determined from long cracks.
Kevinsanny et al. [13] performed tension-compression fatigue tests on two types of Ni-based superalloy 718 with different microstructures (fine grained and coarse-grained) in which small artificial defects of various sizes and shapes were introduced. They showed that the fatigue limit as a small-crack threshold can be predicted using the √area parameter model.

DEFECT PRODUCTION

A set of smooth specimens have been manufactured from Al7475 T7351 aluminium plate, with the final geometry reported into Figure 6. On 10 specimens, a semi-circular flaw 0.36 mm deep representing a defect with target transversal √area of 0.445 mm, was inflicted by Electric Discharge Machining (EDM). Other types of defects listed onto Table 1 have been generated by means of natural and artificial corrosion attack with target transversal √area of 0.445 mm, used for the EDM defect. The number of specimens for each damage type condition are reported in Table 1.

Table 1: Specimens Number for Each Damage Types

Defect Type Methodology	N. of Specimens
Electrical Discharge Machining (EDM):	10
Electrochemical attack (Galvanostatic corrosion):	25
Salt spray fog chamber:	25
Natural marine environment:	15
Natural urban environment:	15

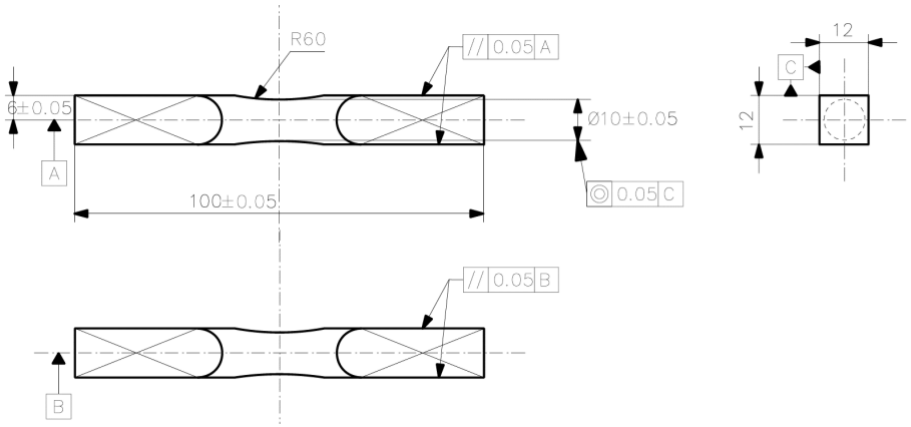

Figure 6: Specimen Dimensions

Each specimen subjected to natural and accelerated artificial corrosion was visually inspected and observed to SEM. A profilometry analysis was then conducted in order to determine the depth and the area of the defect, performed in longitudinal direction as illustrated in Figure 7 due to the cylindrical shape of the specimen; for each defect at least six measures were carried out and the one with the biggest area was considered as the reference. Into the final evaluations, the damage areas have been verified basing on stereo microscope measurements and damage measurement on cross section surfaces on failed specimens.

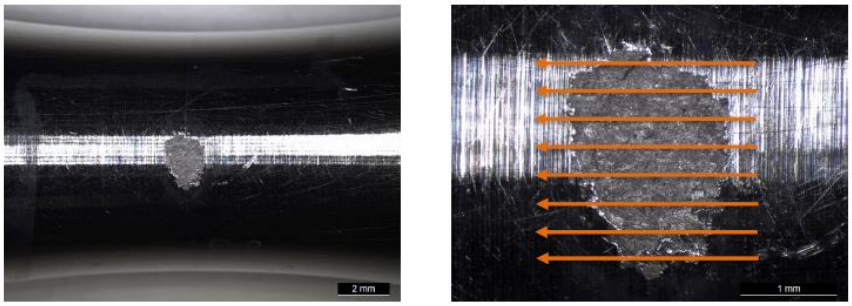

Figure 7: Profilometry Direction

EDM Defect

The EDM defect has a semi-circular shape as shown in Figure 9. The √area of the EDM defects reported in Figure 8 was evaluated as defined in the Eqn. 5, where a and 2c are respectively the flaw depth and length.

$$\sqrt{area} = \sqrt{\frac{1}{2}\pi ac} \tag{5}$$

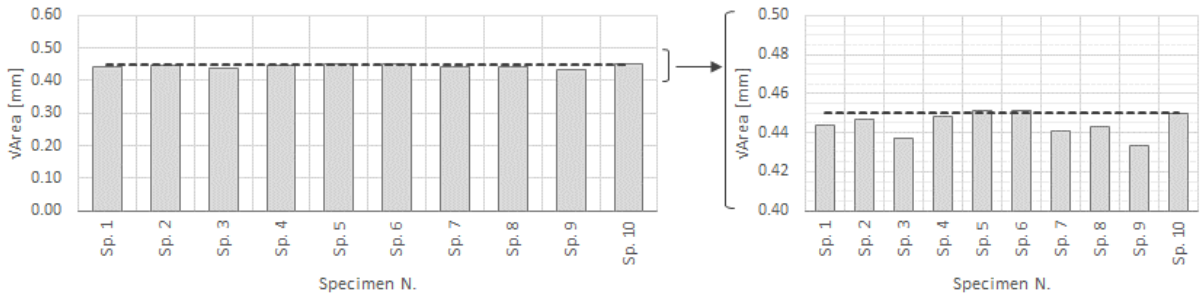

Figure 8: EDM Notch √area vs Target (dotted line: √area=445mm)

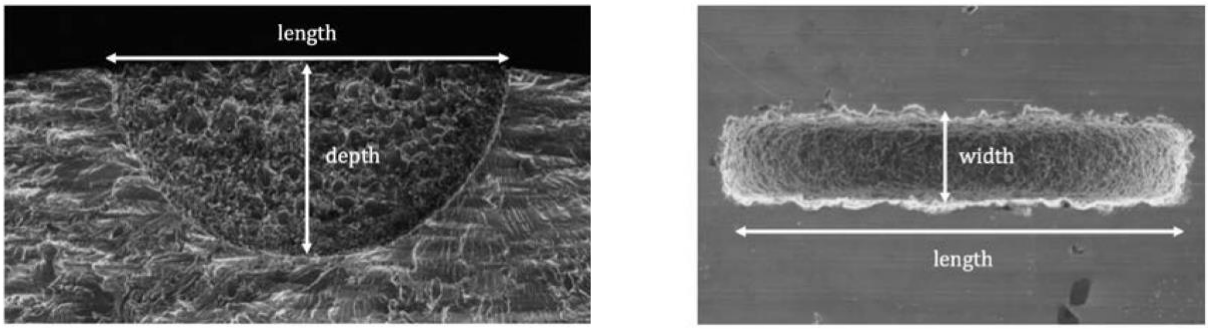

Transverse View Longitudinal View

Figure 9: EDM Notch

Corrosion Defects

Four localized corrosive attacks have been performed:

- controlled corrosive attack (galvanostatic test);
- artificial exposure to salt spray fog chamber;
- natural exposure to urban environment;
- natural exposure to marine environment.

In order to obtain a localized corrosion attack in a specific area of the specimen and with a fixed transversal cross section, the entire surface of the specimen has been protected with the exception of a small area, in order to promote the localization of the corrosion attack.

Two layers of different tapes were used: a transparent water-resistant polyethylene (PE) tape with a 1.4 diameter hole and a black self-amalgamating tape, or electrical insulating tape for salt fog tests, ref. Figure 10 and Figure 11.

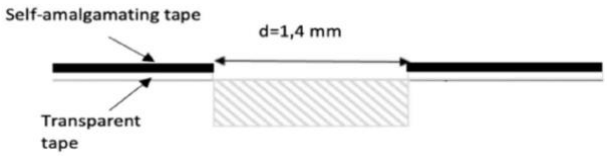

Figure 10: Exposure Area Detail

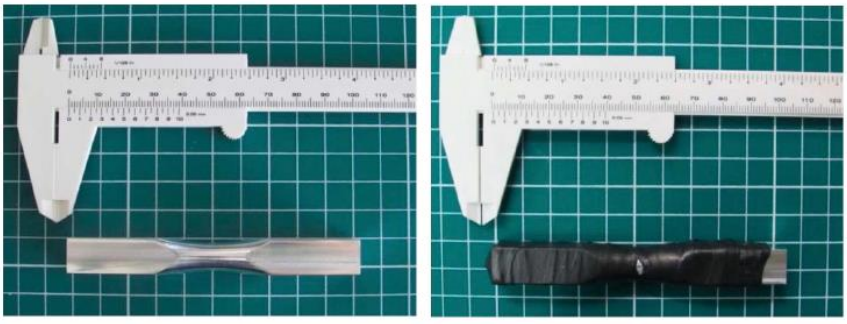

Figure 11: Specimen Before and After Shielding

Electrochemical Galvanostatic Corrosion Test

Galvanostatic tests are performed to generate an artificial well-defined localized corrosion attack [15]. The aluminium specimen is connected to the positive pole of the DC feeder (a galvanostat AMEL Instruments 2049), and a mixed-metal oxide covered titanium mesh (MMO-Ti), used as counter-electrode, is connected to the negative pole. The setup of the test is shown in Figure 12. The aluminium specimen works as anode and its corrosion rate has been controlled by the application of an external

constant current. Specimen and counter-electrode has been immersed in a corrosion cell (1 dm^3) containing distilled water and 5 g/L NaCl.

The application of the Faraday's law allows the calculation of the time required to have a specific mass loss and penetration rate, as defined into Eqn. 6 [15]:

$$t = \frac{\Delta m \cdot z \cdot F}{AW \cdot i \cdot S} \tag{6}$$

where Δm is the mass loss, z is the valence of the anodic reaction, F is the Faraday's constant (i.e. 96485 C), AW is the atomic weight, i is the applied current density, S is the surface and t is the time. A constant anodic current density of 100 $A \cdot m^{-2}$ has been applied, resulting in a test duration of about 10 hours. The √area of the pit corrosion defects is shown in Figure 13.

Figure 12: Setup of the Galvanostatic Test

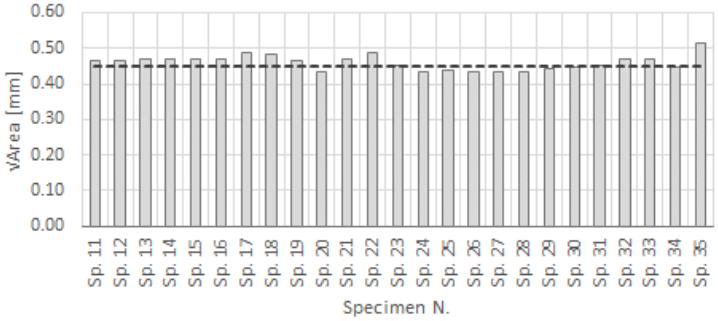

Figure 13: Galvanostatic Corrorion Damage √area vs Target (dotted line: √area=445mm)

Salt Spray Fog Test

The tests were performed in accordance with ASTM B117. Specimens have been exposed to a solution of 5% sodium chloride (NaCl), with a temperature in the range 35 ± 2 °C, and exposed with an angle between 15° and 30° from the vertical for 2 months. Specimens have been visually examined periodically, then re-inserted into the salt spray chamber.

Figure 14 shows that the obtained corroded areas have very heterogeneous dimensions; the salt spray fog has not resulted in predictable and reproducible corrosion attacks.

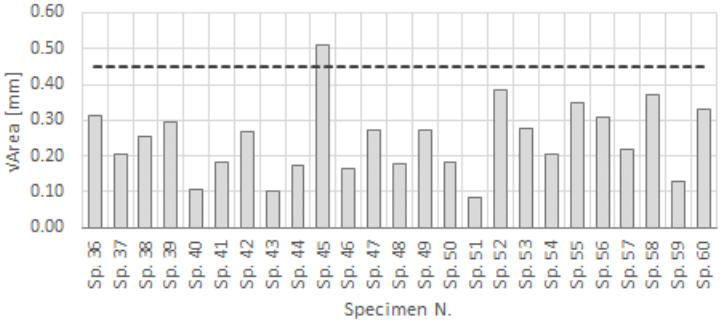

Figure 14: Salt Spray Fog Test Damage √area vs Target (dotted line: √area=445mm)

Natural Exposure to Urban Atmosphere

Test were performed on the roof of the Department of Chemistry, Materials and Chemical Engineering "Giulio Natta" of Politecnico di Milano (Milan, Italy). Specimens have been exposed for 1 year on a

rack, South-Est oriented, direct open air and exposed with an angle between 40° and 45° from the vertical to all atmospheric conditions and atmospheric contaminants.
At the end of the year of exposure, all the samples were disassembled for a visual and a stereomicroscopy inspection. Some dark coloured spots were identified on few specimens (# 69, #70 and # 73). To confirm or exclude the formation of corrosion attacks, they were completely uncovered, pickled in nitric acid and subjected to profilometry. The results confirmed the total absence of localized corrosion attacks of significant depth (ref. Figure 15 as example, referred to specimen 69). The dark spots can therefore be attributed to the deposition of particulate matter on the exposed areas, which were completely removed by the pickling operation.

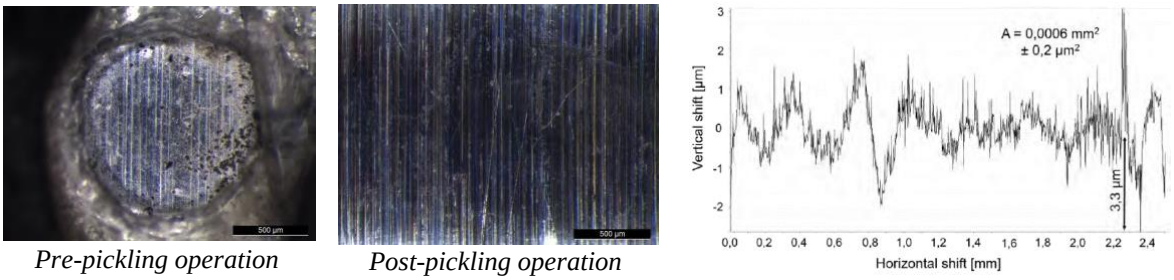

Figure 15: Specimen 069 Analysed After One Year; Stereo and Profile Images

Natural Exposure to Marine Atmosphere
Tests have been performed at CNR laboratory in Bonassola (La Spezia, Italy).
All specimens have been open-air, direct exposed in the direction of the sea for 1 year to all atmospheric conditions and atmospheric contaminants. Specimens have been placed on a rack, at a distance of 20 cm from each other, and exposed with an angle between 30° and 35° from the vertical. The elevation of the exposure point above the mean sea level is 6 m, the distance between exposure point and sea is about 15 m, and the exposure orientation is E-SE, as shown in Figure 16. A macroscopic weekly observation with a monthly report has been carried out.

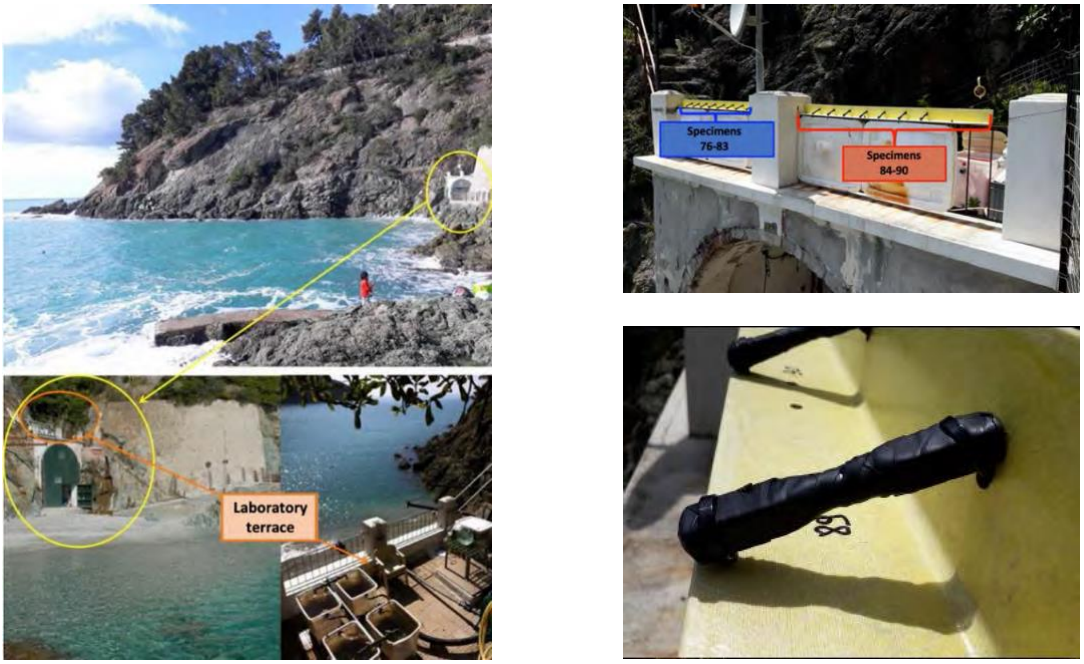

Figure 16: Exposure Rack on the Terrace of MARECO CNR-ICMATE Laboratory

At the end of one year of exposure, several small corrosion attacks were detected on all the specimens. The stereomicroscopy analysis also shows scratches produced accidentally in Bonassola, probably due

to an unsuccessful attempt to re-open the self-amalgamating tape (that has the tendency to close on itself). The results of laser profilometry are shown in Figure 17; the minimum, maximum and average depth of the attack is reported, measured on at least 6 profiles made on each specimen.

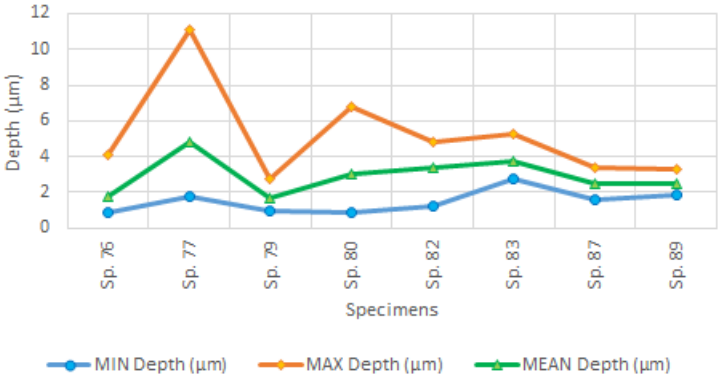

Figure 17: Natural Exposure to Marine Environment

FATIGUE TESTS

The experimental tests consist in the determination of the fatigue endurance limit of Al7475 T7351 specimens in presence of a defect, for a constant stress ratio of R=0.1. The limit is obtained using the Hodge-Rosenblatt simplified stair case statistical method [16] which consists of a sequence of tests at increasing or decreasing stress levels, where the decision to use an increasing or decreasing level for the "next" test depends on the results (run out or failure) of the current test. Finally, the endurance limit is obtained as an average of the value of the stress levels applied plus an additional fictitious point. Fatigue tests are performed for each type of defects, selecting the specimens in order to have a nominal value of √area as close as possible to the target value of 0.445 mm. Fatigue tests on natural corrosion - urban environment specimens have not been performed because no significant localized corrosion attacks have been obtained. Fatigue tests on natural corrosion – marine environment specimens have been performed for a smaller defect size, since none of them was able to reach the target value of √area = 0.445 mm.
The alternate bending fatigue test have been executed on a RUMUL testing apparatus. The defect generated by corrosion may have different geometries, but it is always located in the centre of the specimen. Runout was set at 10 million cycles. Ten specimens have been tested for each defect type.

EDM Defect

Figure 18 shows a typical section failure with a detail of the EDM defect.

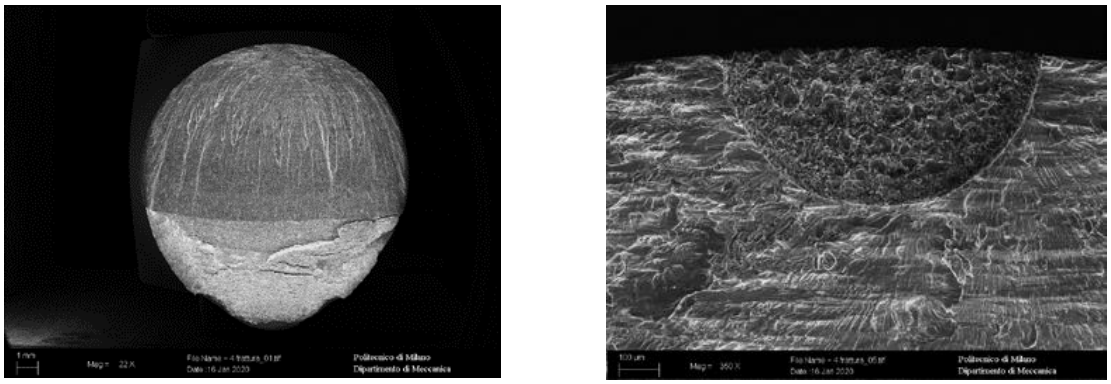

Figure 18: Fracture Surface of EDM Defect

Accelerated Corrosion Pit (Galvanostatic Corrosion)

A statistical analysis Galvanostatic Corrosion pit dimensions have been performed, in order to select at least 10 specimens which best represent the 10 EDM specimens in terms of √area. The subset has been defined in order to have the value of √area as close as possible to the EDM mean value, excluding from stereomicroscope measurements specimens where the flaws have a 2c/a ratio greater than 10 since, according to Murakami, above this ratio the stress intensity factor tends to a constant value despite the area increase, and an effective √area needs to be estimated following different rules. The average √area of the tested specimens is 457 μm.

Figure 19 shows a typical section failure with a detail of the Galvanostatic Corrosion defect.

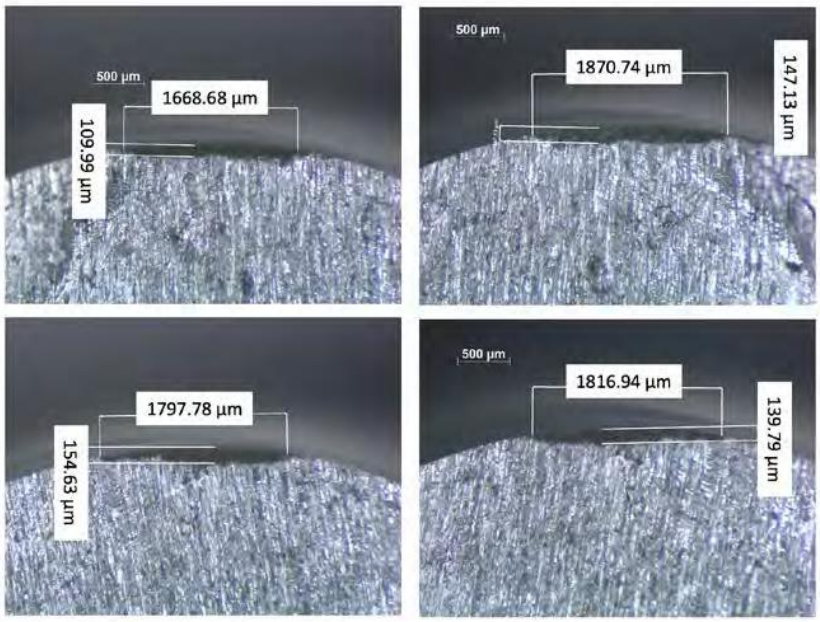

Figure 19:Stereomicroscope Evaluation of the Galvanostatic Corrosion Defect (the two sides of two specimens are reported)

Accelerated Corrosion Pit (Salt Spray Corrosion)

Salt spray corrosion defects have highly irregular shapes; in these cases the method suggested by Murakami and displayed in Figure 4 has been adopted evaluating the √area of the half ellipse circumscribing the defect in order to select at least 10 specimens. The rules adopted for the selection of the representative sub-set are the same adopted for Galvanostatic Corrosion. The average √area of the tested specimens is 390 μm.

Figure 20 shows a typical section failure with a detail of the Salt Spray Corrosion defect.

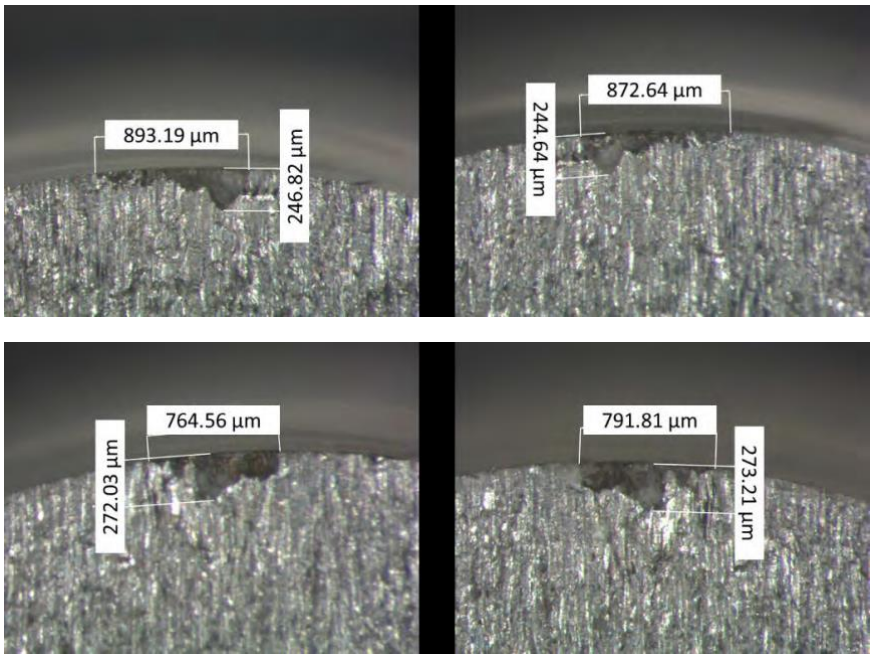

Figure 20: Stereomicroscope Evaluation of the Salt Spray Corrosion Defect (the two sides of two specimens are reported)

Natural Corrosion Pit (Marine Environment)

The profilometry revealed that the depth of attack is less than 5 µm. Accordingly, the profilometry measured transversal area is meaningless since these values are comparable with the sample surface roughness. Furthermore, stereomicroscope observations revealed the presence of scratches on several coupons. 10 specimens were selected for the testing, eight without scratches and two with the smallest scratches after verifying that the crack started from the corrosion pit. The actual corrosion pit dimensions were measured on failed specimen, resulting in an average √area of 82.07µm.

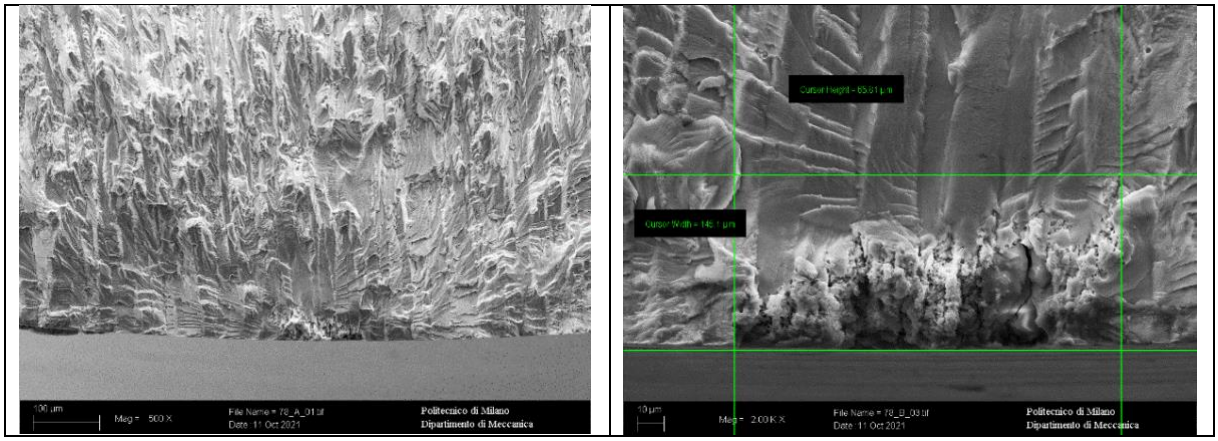

Figure 21: SEM Observations of Natural Corrosion Pit

TEST RESULTS

The results of the Hodge Rosenblatt sequences for the four types of tested damage types is shown in Figure 22; artificial corrosion and EDM defects, have the same fatigue strength.

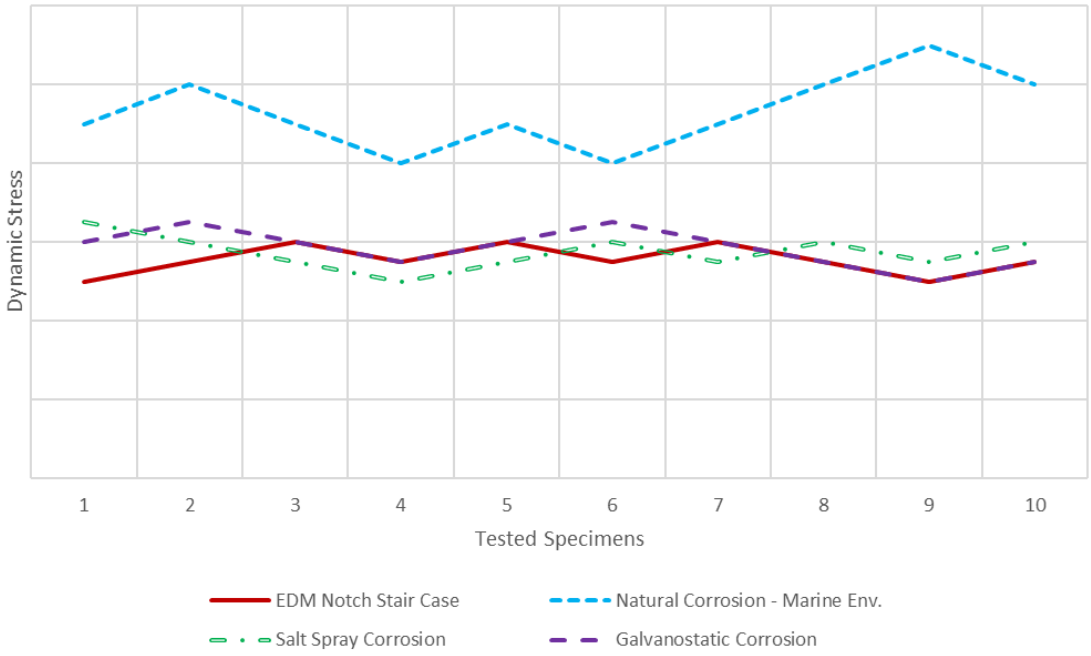

Figure 22: Comparison of Stair Case Sequences

Natural corrosion pits are significantly smaller and thus not directly comparable with EDM flaws or artificial corrosion pits; for this reason, they are compared, in terms of El/Haddad model, with the Kitagawa plot obtained during a comprehensive material characterization carried out in the past on the same material but with a different type of artificial defect (two micro-holes, Figure 23), whose aim was to obtain the threshold to crack propagation curves (Kitagawa plots) with varying the stress ratio and the flaw size [17].
As shown in Figure 24, the fatigue strength of natural corrosion specimens are in a good agreement with the Kitagawa curve previously obtained, confirming also in this case the equivalence between the fatigue behaviour of the defects generated by natural corrosion an those obtained with the mechanical processes used for the material characterization in terms of threshold to crack propagation.

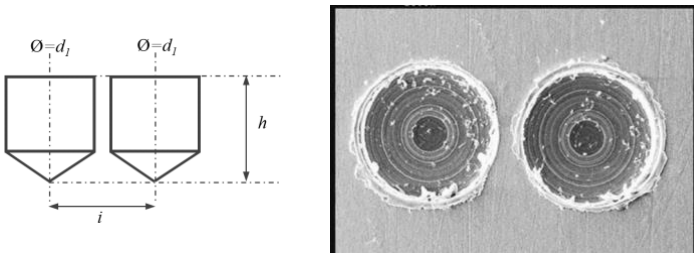

Figure 23: Defect Geometry used into Ref. [17]

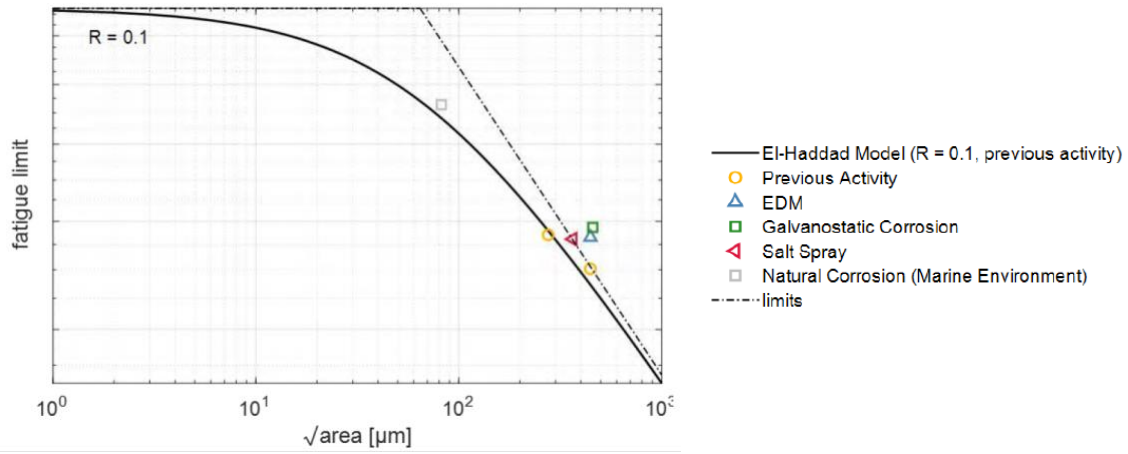

Figure 24: El-Haddad Model of Previous Activity [17] and Current Activity Results

CONCLUSION

The aim of the research activity is to evaluate the fatigue limit of Al7475 T7351, in alternate bending (R = 0.1), in presence of a defect with √area = 0.445 mm, comparing results from EDM flaw with different types of corrosion defects:

- accelerated corrosion pit (galvanostatic corrosion)
- accelerated corrosion pit (salt spray corrosion)
- natural corrosion (urban environment)
- natural corrosion (marine environment)

EDM flaw is considered as the base case study and corrosion pits have been generated to obtain the same value of √area. Galvanostatic corrosion proved to be a reliable method to obtain a corrosion pit of the target dimension, even if it does not reach the same level of repeatability of pit dimensions compared with EDM flaw, and a statistical approach has been followed to select the best specimen population to perform fatigue tests. Salt spray corrosion has been the less controllable process, but it allowed to obtain a selection of specimens with pit dimensions comparable to EDM flaw. Natural corrosion is not controllable and, after one year of exposure, it has not been possible to obtain the target pit dimension. In particular: specimens exposed to urban environment do not show significant corrosion, while specimens exposed to marine environment generated corrosion pits of much smaller size. With respect to damage shape, EDM flaw geometry is hemispherical while corrosion pits geometries are typically elliptical with higher value of 2c/a.
The results of the activity show a strong correlation among the threshold to propagation from accelerated corrosion, natural corrosion and the artificial flaws, confirming the applicability of Kitagawa diagrams derived from artificial defects inflicted with the reported methodologies to describe the damage tolerance behaviour in presence of corrosion pits of equivalent √area. More in details, obtained results demonstrate that fatigue material behaviour in presence of a corrosion pit, either from natural and accelerated process, when subjected to fatigue loads is equivalent to results obtained with artificial defects inflicted by Electrical Discharge Machining (EDM) of the same √area; fatigue behaviour of natural corrosion specimens, that resulted in a smaller value of √area, are well in accordance with the traced El-Haddad model of the Al7475 T7351 of Figure 24 based on a different process used to inflict a damage (Figure 23).

REFERENCES

[1] N. Larrosa, R. Akid and R. Ainsworth, «Corrosion-Fatigue: a Review of Damage Tolerance Models,» International Materials Reviews, vol. 63, n. 5, pp. 283-308, 2018.
[2] H. Kitagawa and S. Takahashi, «Applicability of Fracture Mechanics to Very Small Cracks or Cracks in the Early Stage,» in Proceeding of the Second International Conference on Mechanical Behavior of Materials, ASM , 1976.
[3] J. Maierhofer, H. -P. Ganser and R. Pippan, «Modified Kitagawa-Takahashi Diagram Accounting for Finite Notch Depths,» International Journal of Fatigue, n. 70, pp. 503-509, 2017.
[4] Y. E. M. Murakami, «Effect of Hardness and Crack Geometries on ΔKth of Small Cracks Emanating from Small Defect,» in Mechanical Engineering Publications, Miller KJ, de Los Rios ER, editors, 1986, pp. 275-293.
[5] S. W. Smith, J. A. Newman and R. S. Piascik, «Simulation of Fatigue Crack Initiation at Corrosion Pits with EDM Notches. Report No. L-18262,» 2003.
[6] B. M. Schonbauer and H. Mayer, «Effect of Small Defects on the Fatigue Strength of Martensitic Stainless Steels,» International Journal of Fatigue, n. 27, pp. 362-375, 2019.
[7] B. M. Schonbauer, S. E. Stanzl-Tschegg, A. Perlega, N. Salzman, N. F. Rieger, S. Zhou, A. Turnbull e D. Gandy, «Fatigue Life Estimation of Pitted 12% Cr Steam Turbine Blade Steel in Different Environments and at Different Stress Ratios,» n. 65, pp. 33-43, 2014.
[8] S. B. Li, W. P. Zhang, X. L. Gu e C. M. Zhu, «Analysis on Fatigue of Natural Corrosion Steel Bars,» Advanced Materials Research, Vol. %1 di %2163-1677, pp. 3237-3241, 2010.
[9] Y. Murakami and B. M. Endo, « Effects of defects, inclusions and inhomogeneities on fatigue strength » International Journal of Fatigue, n. 16, pp. 163-182, 1994.
[10] Y. Murakami, Metal Fatigue: Effects of Small Defects and Nonmetallic Inclusions, Elsevier, 2002.
[11] M. H. El Haddad, T. H. Topper e S. K. N., «Prediction of Non Propagating Cracks,» Engineering Fracture Mechanics, vol. 11, n. 3, pp. 573-584, 1979.
[12] B. M. Schonbauer, K. Yanase and M. Endo, «Influence of Intrinsic and Artificial Defects on the VHCF Properties of 17-4PH Stainless Steel,» Procedia Structural Integrity, n. 2, pp. 1149-1155, 2016.
[13] Kevinsanny, S. Okazaki, O. Takakuwa, Y. Ogawa, K. Okita, Y. Funakoshi, J. Yamabe, S. Matsuoka e H. Matsunaga, «Effect of Defects on the Fatigue Limit of Ni-Based Superalloy 718 with Different Grain Sizes,» Fatigue & Fracture of Engineering Materials & Structures, vol. 42, n. 5, pp. 1203-1213, 2019.
[14] B. M. Schonbauer, K. Yanase and M. Endo, «The Influence of Various Types of Small Defects on the Fatigue Limit of Precipitation-Hardened 17-4PH Stainless Steel,» Theoretical and Applied Fracture Mechanics, n. 87, pp. 35-49, 2017.
[15] P. Pedeferri, Corrosion Science and Engineering, Springer, 2018.
[16] A. Brand and R. Grégoire, Donnéès Technologiques sur la Fatigue, CETIM, 1991.
[17] Politecnico di Milano, Determinazione dello stato tensionale in componenti meccanici dell'elicottero AB 139 e svolgimento di prove sperimentali di limite di fatica con difetto, 2006.